Optimum mobility, contact properties, and open-circuit voltage of organic solar cells: A drift-diffusion simulation study

Wolfgang Tress,* Karl Leo, and Moritz Riede
Institut für Angewandte Photophysik, Technische Universität Dresden, George-Bähr-Str. 1, 01069 Dresden, Germany
(Received 22 December 2011; published 4 April 2012)

We investigate the role charge carrier mobility plays for loss mechanisms in organic bulk heterojunction solar cells. For this purpose, we perform drift-diffusion calculations for several recombination models and properties of the contacts. We show that in case of selective contacts, higher mobilities increase device efficiency, independent of injection barrier heights, energy level bending at the contacts, and the amount of background dark carriers in the device. Nonselective contacts provide a source of photocarrier loss at the "wrong" electrode. This is evident from a decrease of the open-circuit voltage (V_{oc}) with an increased role of charge carrier diffusion, which originates from a higher mobility or from interface barriers reducing the built-in potential. In this case, V_{oc} furthermore depends on the device thickness. Considering the effect of different recombination models, a too high mobility of one charge carrier decreases V_{oc} significantly for Langevin recombination. That is why balanced mobilities are desirable for high efficiency in this case. In presence of recombination via CT states, V_{oc} is mainly governed by the dynamics of the charge transfer state. Based on these differentiations we show that the existence of an optimum mobility derived from simulation depends strongly on the assumptions made for contact and recombination properties and obtain a comprehensive picture how charge carrier mobility influences the parameters of organic solar cells.

DOI: 10.1103/PhysRevB.85.155201 PACS number(s): 88.40.jr, 84.60.Jt, 73.50.Gr

I. INTRODUCTION

Organic solar cells have shown an impressive improvement based on intensive research and development in the last decade: device efficiencies increased from 3% to close to 10%.[1] A tailored material synthesis has lead to a variety of novel absorber and transport materials, which allow for a higher variability and flexibility in the device design. However, the performance of organic solar cells is determined by a multitude of device parameters. Combined with the multilayer design, usually including mixed layers, experimental device optimization toward highest efficiency is a challenging task. Thus simulations specifying criteria for high-performance devices are of key importance.

Drift-diffusion modeling of organic solar cells has been demonstrated to be a powerful tool[2,3] to explain the influence of various effects on the current-voltage characteristics (J-V curve). In addition to reproducing and explaining experimental data, these simulations can be employed predictively to define requirements of desired material properties.

One major material property with significant influence on device efficiency is the charge carrier mobility μ in an organic bulk heterojunction (BHJ) solar cell. Such a solar cell consists of a blend of two materials, donor and acceptor.[4–7] Light absorption takes place on one or ideally on both components by creating a molecular excited state. This state migrates diffusively and can be efficiently separated into a free charge carrier pair at a heterojunction. Subsequently, the electron is extracted from acceptor domains and the positive charge (hole) from the donor material. Under the assumption of an intimate intermixing with still existing pathways the blend may be considered as one effective medium. In this approach, the energy levels charges are transported on are defined by the pristine material properties, as long as polarization effects do not significantly change upon blending. Thus the ionization potential (IP), defining the valence state energy (hole transport level) of the film, is determined by the donor, and the electron affinity (EA) as electron transport level by the acceptor. The energy gap is then an effective gap E_g^{DA} between the EA of the acceptor (A) and the IP of the donor (D) and has to be distinguished from the optical gap determined by the onset of absorption of the absorber molecule(s). Charge carrier mobilities are functions of the hopping rates between donor (or acceptor) molecules and depend strongly on the morphology of the intermixed layer. The main advantage of this effective medium approach is the possibility to perform a one-dimensional simulation of a BHJ as a single layer between metal contacts[2] in order to evaluate the effect of μ, although being aware of the fact that μ is an effective parameter.

Several modeling studies on the impact of μ on device performance have been reported in literature,[8–13] mostly claiming the existence of an optimum (finite) value of μ. The specific motivation for such μ-dependent studies in organic materials is the correlation of mobility and recombination in Langevin theory.[14] In this theory, the field-dependent charge carrier extraction probability governed by μ is directly competing with the diffusion-limited recombination, which is thus also increased for increasing mobility. The studies in literature consider different aspects and found different reasons for the fact that too high mobilities might be detrimental for the device performance, seen in a decrease in open-circuit voltage (V_{oc}). Wang *et al.*[10] and Shieh *et al.*[11] claim recombination with dark charge carriers injected from the contacts to be responsible for a decrease in V_{oc}, because their density increases with μ. Mandoc *et al.*[8] and Deibel *et al.*[9] state that a high mobility accompanied by too fast charge carrier extraction reduces V_{oc}. Wagenpfahl *et al.*[12] separate the two processes charge extraction and recombination by using a capped Langevin recombination that results in a maximum of the efficiency for high μ.

Here, we show that the existence of an optimum mobility is strongly determined by the conditions assumed for the simulations. We perform drift-diffusion calculations for several recombination models and properties of the contacts and consistently explain all observed features starting from fundamental equilibrium conditions. We estimate how realistic the existence of a (not yet experimentally confirmed) optimum mobility is and outline possibilities on how to find limiting mechanisms by experiment. Furthermore, by a systematic approach and analytical equations, we clarify several points that were not fully elaborated in existing studies.

II. MODELS AND METHODS

A. Mobility and recombination models

In organic materials where hopping transport is dominant, the mobility has to be seen as a relatively macroscopic, effective parameter, relating the effective drift velocity v to the electrical field E via $v = \mu E$. Thus a constant μ implies a linear relation between v and E. More realistic models include a field, temperature, and charge carrier density dependence,[15] which we omit here for reasons of clarity and comprehensibility. According to the mentioned definition, one would expect that the mobility of the active material is not important for solar cell performance, because it solely determines the velocity of charge carriers at a certain field, and, thus the response time of the device that is irrelevant for solar cells working in steady state. However, the mobility is important for charge extraction, which itself has always to be seen in relation to the competing mechanism of recombination. The equilibrium between charge carrier recombination, generation, and extraction, which is influenced by the applied bias, defines the dependence of the photocurrent on voltage, which is mainly seen in the fill factor (FF) and for very low values of the FF in the short-circuit current density as well. A higher μ increases charge carrier extraction, and therefore should always be beneficial for the FF and, consequently, for the efficiency η, as long as μ does not influence recombination rates.

In a BHJ, there exist two possibilities where μ can change recombination properties and thus introduce losses: μ can influence either surface recombination of a charge carrier at the "wrong" electrode (hole at cathode, electron at anode) or recombination at a donor-acceptor interface in the material itself, which we call bulk recombination. The latter can be described by several models presented below.

1. Direct and Langevin recombination

Direct electron-hole recombination R_0 is governed by both charge carrier densities n (electrons) and p (holes):

$$R_0 = \beta\left(np - n_{\mathrm{i}}^2\right) \tag{1}$$

with the recombination constant β and the intrinsic charge carrier density n_{i}. Langevin theory[14] gives a description of β as a function of μ:

$$\beta_{\mathrm{L}} = \frac{e(\mu_n + \mu_p)}{\epsilon_0 \epsilon_{\mathrm{r}}}. \tag{2}$$

Here, μ_n is the electron mobility, μ_p the hole mobility, $\epsilon_0\epsilon_{\mathrm{r}}$ the permittivity of the material, and e the elementary charge. This recombination R_0 is also called bimolecular because it requires two free charge carrier species. Commonly, a lower β than predicted by Langevin theory is observed in experimental data of BHJs that lead to the proposal by Koster *et al.*[16] to replace the sum of the mobilities by $\min(\mu_n,\mu_p)$. The reason why the slower charge carrier limits β is supposed to be the phase separation requiring both charge carriers to travel to a heterointerface in order to recombine.

However, there is no clear evidence of Langevin recombination in experimental data of small molecule solar cells. For example, β seems not to be affected in BHJs with different mixing ratios, although mobilities change significantly.[17] That is why a mobility independent β can also be a reasonable choice.

2. Geminate recombination or recombination via CT states

In the case of geminate recombination, the consequences of a so-called charge transfer (CT) state are considered. This bound electron/hole pair with binding energy E_{B} is an intermediate state, excitons are supposed to pass through when being dissociated and charge carriers when recombining. The CT dissociation and recombination are proportional to its density X and described by the rates k_{diss} and k_{relax}. This leads to a modification of free charge carrier generation ($G_0 \rightarrow G$) and recombination terms by P, which describes the probability of the dissociation of a CT state:

$$G = G_0 P \tag{3}$$

and

$$R = R_0(1 - P), \tag{4}$$

where G_0 is the generation rate of CT states, G (R) is the effective generation (recombination) rate of free charge carriers, and P is given under the assumption of no other drain terms for CT excitons by

$$P = \frac{k_{\mathrm{diss}}}{k_{\mathrm{diss}} + k_{\mathrm{relax}}}. \tag{5}$$

Here, k_{diss} satisfies the following equation:

$$k_{\mathrm{diss}} = \beta e^{-\frac{E_{\mathrm{B}}}{k_{\mathrm{B}}T}} f(E, E_{\mathrm{B}}). \tag{6}$$

These equations together with the description of the field(E)-dependent function $f(E,E_{\mathrm{B}})$ constitute the Onsager-Braun model.[2,18,19] The proportionality of k_{diss} in Eq. (6) to the bimolecular recombination constant β of Eq. (1) results directly from the detailed balance condition $k_{\mathrm{diss}} X_0 = \beta n_{\mathrm{i}}^2$ with the equilibrium densities for CT states X_0 and free charge carriers n_{i}, which are defined by the relaxation/recombination dynamics of the single species at a certain temperature. According to Eq. (6), the dissociation of the CT state is assumed to be temperature activated with the binding energy E_{B} as activation energy. The significance of a CT state can be seen in experiment at a strongly pronounced electrical field and characteristic temperature dependence of the photocurrent, as, e.g., observed in Ref. 20.

3. Trap-assisted recombination

Recently, indirect recombination has increasingly been proposed as the dominating loss mechanism in organic solar cells.[21,22] To discuss this qualitatively, we consider a

simple trap-assisted Shockley-Read-Hall (SRH) expression[23] for midgap traps with density N_t and the same capture coefficient c_t for electrons and holes:

$$R_{\mathrm{SRH}} = c_t N_t \frac{np - n_i^2}{n + p + n_1 + p_1}. \tag{7}$$

In conventional theory, c_t is proportional to the thermal velocity and a cross section.[23] N_t is the trap density and n_1 and p_1 are characteristic charge carrier densities. In the case of midgap traps, they are very low compared to the amount of photogenerated charge carriers. Charge carriers recombining via traps are directly lost. Here, we do not consider the possibility of a formation of a bound electron/hole pair as we did in the case of direct recombination. The reason is that, if such a state is formed, its dissociation probability is supposed to be very low due to the assumptions of deep traps that are very unlikely to release charge carriers after having trapped them.

B. Contact Properties

For the simulation study, we assume the BHJ to be sandwiched between two metal contacts. The position of the anode is set to zero and the position of the cathode to d according to the sketch in Fig. 1. The current or the charge carrier densities at the contacts are described by a simple temperature activated injection model with the injection barriers φ as difference between the charge transport levels and the metal work function. The surface current J_s can then be written (here for electrons) as

$$J_s = (n - n_0)s_n = \left[n - N_C \exp\left(-\frac{\varphi_n}{k_B T}\right)\right] s_n, \tag{8}$$

where s_n is the surface recombination velocity and n_0 the equilibrium charge carrier density defined by the effective density of states N_C and the barrier φ_n.

We consider a sufficient majority charge carrier extraction, which is given for a metal/organic contact of working solar cells. This means $s \to \infty$ and thus $n(d) = n_0(d)$ and $p(0) = p_0(0)$. These conditions say that the contacts are in equilibrium independent of the working point of the device because all excess charge carriers are instantaneously extracted. The same holds for the injection of charge carriers if $n(d)[p(0)]$ tend to values smaller than the equilibrium density $n_0(d)[p_0(0)]$. The case of a reduced majority carrier extraction velocity or probability, which might result from some insulating layer between metal and active material, is not discussed here. Instead, it is referred to Refs. 3 and 12 for experimental and simulation results on that topic. Commonly, the terms "majority" and "minority" are known from doped layers. Here, they refer to the concentrations in an intrinsic BHJ close to the contacts. Therefore electrons are defined as majorities at the cathode and holes at the anode as long as $\varphi < E_g^{\mathrm{DA}}/2$ (cf. Fig. 1).

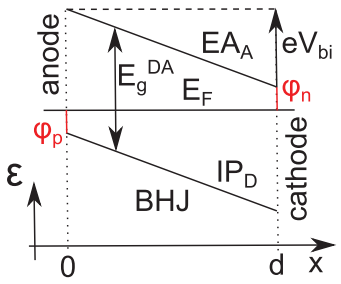

FIG. 1. (Color online) A bulk heterojunction (BHJ) as effective medium between two metal contacts, determining the built-in potential V_{bi}. Offsets between charge carrier transport levels and the metal work function (including potentially present dipoles) are injection barriers φ. The effective gap E_g^{DA} is the difference between the ionization potential of the donor ($\mathrm{IP_D}$) and the electron affinity of the acceptor ($\mathrm{EA_A}$).

The selectivity of the contact is defined by the extraction velocity of charge carriers, reaching the "wrong" contact. These are electrons at the anode and holes at the cathode, which we call minority charges, because their equilibrium densities at these contacts are very low due to the large injection barrier $E_g^{\mathrm{DA}} - \varphi_p$ ($E_g^{\mathrm{DA}} - \varphi_n$). For nonselective contacts, we set $s \to \infty$, and thus $p(d) = p_0(d)$ and $n(0) = n_0(0)$. Selective contacts mean a perfect blocking of the minorities, which results in surface recombination velocities $s_p(d) = 0$ and $s_n(0) = 0$. Usually, metal contacts are nonselective, because both types of charge carriers are extracted. In real devices, selective contacts are achieved by introducing passivation or blocking layers between metal and active material.

The built-in potential V_{bi}, as the difference between anode and cathode work functions, can equivalently be expressed according to Fig. 1 by E_g^{DA} and the injection barriers:

$$V_{\mathrm{bi}} = E_g^{\mathrm{DA}} - \varphi_n^{\mathrm{cathode}} - \varphi_p^{\mathrm{anode}}. \tag{9}$$

C. Studied cases

To investigate the interplay between mobility and recombination, we discuss mobility variations for several recombination models and contact conditions, which can be present in real devices. They are summarized here for the sake of clarity with the aid of Fig. 2:

(1) direct (bimolecular) recombination according to Eq. (1) where we distinguish between three cases: (i) β is constant, (ii) β depends on μ according to Langevin theory [see Eq. (2)], and (iii) β depends on $\min(\mu_n, \mu_p)$ according to the proposal by Koster *et al.*[16]

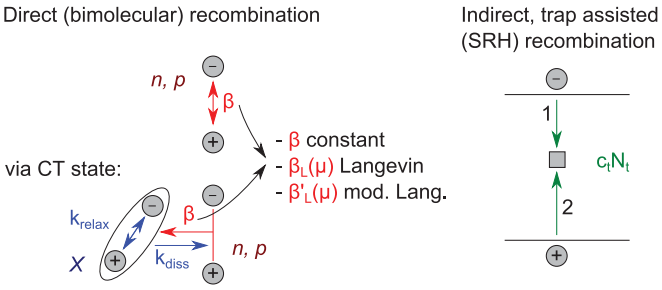

FIG. 2. (Color online) Schematic visualization of the studied recombination processes: Left: direct recombination between electron n and hole p (bimolecular) with different models for the recombination constant β. Direct "recombination" into a CT state, with relaxation k_{relax} and dissociation rate k_{diss}. Photogenerated excitons, entering the CT state, can recombine geminatly. That is why this recombination via CT-states is also called geminate recombination. Right: indirect, trap-assisted (SRH) recombination.

(2) Recombination via CT states and geminate recombination [see Eqs. (3)–(6)]. The "recombination" rate R_0 of free charge carriers into a CT state can be described by the three models mentioned above. Additionally to one distinct CT state, a distribution of E_B can be considered.[20] Here, we restrict ourselves on showing simulation data of recombination via one distinct CT state with binding energy E_B. Furthermore, we select β according to Langevin theory to describe the rate of free charge carriers forming this CT state.

(3) Trap assisted/ indirect (SRH) recombination according to Eq. (7) where we select for the parallel mechanism of direct recombination the case of a constant and low $\beta = 7.23 \times 10^{-11}$ cm^{3}s^{-1} to focus on the influence of indirect recombination.

All these recombination mechanisms can be studied in combination with selective and nonselective contacts and in the case of "low" (0.1 eV) and "high" (0.3 eV) injection barriers. As we focus on trends and their explanations, only data of the most interesting combinations of the presented models and contact properties are shown.

The drift-diffusion simulation, which numerically solves continuity and Poisson equations,[2,3] requires further input parameters, which are summarized in Table I. The conclusions of this paper are not sensitive to these further parameters. Mainly, absolute values will shift, e.g., photocurrents linearly with G_0 and d, and V_{oc} with E_g^{DA} and $N_{C/V}$. A change of ± 2 of ϵ has minor effects. Larger values of d require higher μ to reach the same solar cell performance. However, as all plots show μ in a logarithmic scale, also this influence does not significantly change the presented results.

TABLE I. Standard input parameters for the simulations shown. The values might represent the properties of a ZnPc:C_{60} bulk heterojunction solar cell.

parameter	value
E_g^{DA}	1.2 eV
$N_C = N_V$	10^{21} cm^{-3}
ϵ_r	5
d	50 nm
G_0	1.5×10^{22} cm^{-3}s^{-1}
$\varphi_n = \varphi_p$	0.1 or 0.3 eV
T	300 K

III. RESULTS AND DISCUSSION

A. Recombination only in the BHJ (selective contacts)

We start with the case of nonsignificant injection barriers and selective contacts, where a loss via surface recombination is excluded. Figure 3 shows the efficiency η as a function

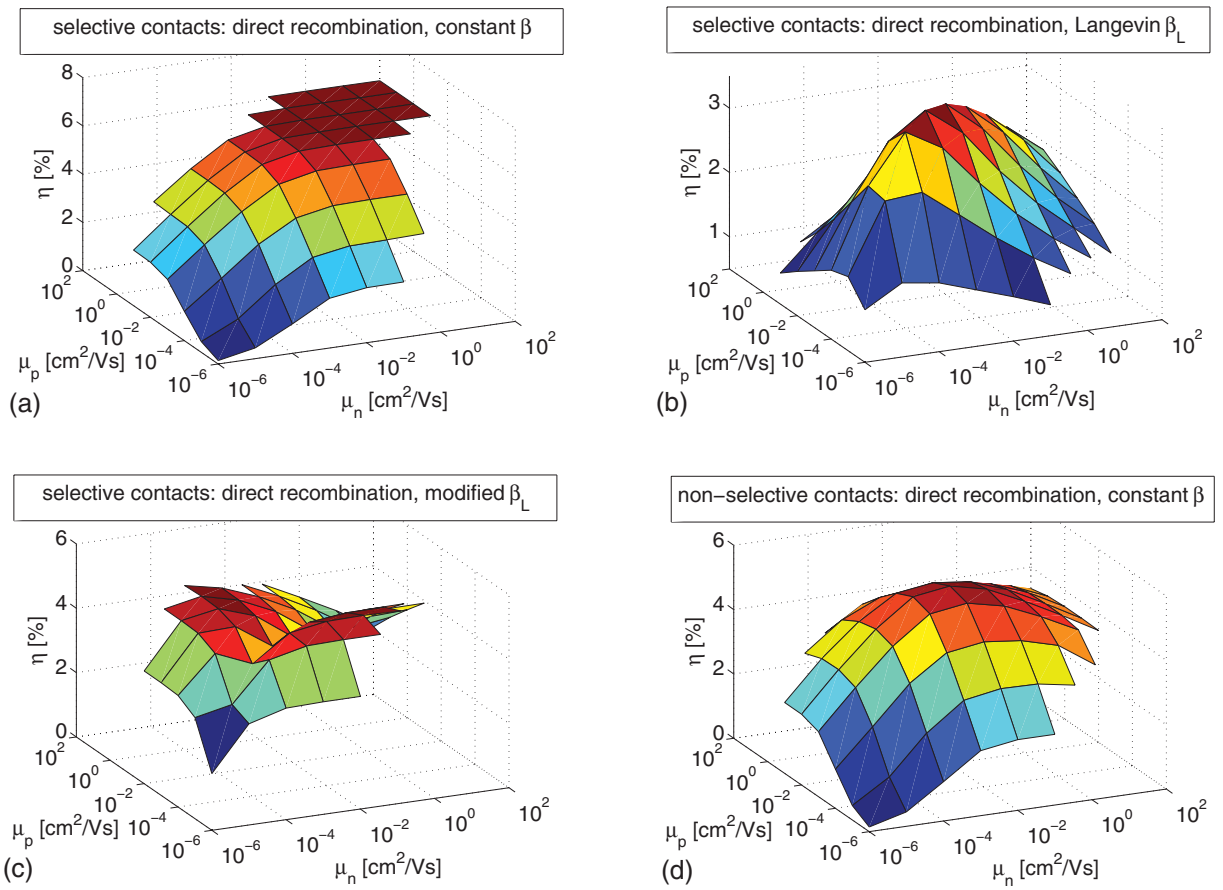

FIG. 3. (Color online) Efficiency η as a function of electron and hole mobilities μ_n and μ_p for different recombination models and contact properties: (a)–(c) selective contacts with (a) constant β (qualitatively similar to Langevin recombination via a distinct CT state), (b) direct Langevin recombination (c) same as case (b), but with a modified $\beta \propto \min(\mu_n, \mu_p)$. (d) Same as case (a), but for nonselective contacts.

of electron and hole mobility for the different recombination models. In case of direct recombination with a constant recombination coefficient β [see Fig. 3(a)], the efficiency increases with mobility of each charge carrier type independently of the mobility of the other one. This is due to an increased charge carrier collection reaching a saturation at $\mu \approx 10^{-2}$ cm^2/Vs. The absolute value of η depends on the choice of β (here 7.23×10^{-11} cm^{3}s^{-1}). In the case of Langevin recombination [see Fig. 3(b)], balanced mobilities are found to be beneficial, as proposed, e.g., in a recent modeling study.[24] The reason is that the recombination constant is dominated by the faster charge carrier [see Eq. (2)], whereas a sufficient charge carrier extraction always relies on the extraction of both charge carriers. Thus it is limited by the slower one. Although the faster charge carrier can compensate for the slower one to some extent by creating a space charge[25,26] and hence selectively increase the field and thus the probability of the slower one to be extracted, the FF is reduced by the imbalance in mobilities. Interestingly, there exists an optimum value for balanced mobilities ($\mu_n = \mu_p = 10^{-3}$ cm^2/Vs), above which the efficiency drops. This effect will be discussed subsequently.

Figure 3(c) shows η as a function of mobilities under the assumption of a modified β according to Koster *et al.*[16] It can be seen that an exact balance in μ is detrimental, because the recombination is dominated by the slower charge carrier, whereas extraction can be enhanced by increasing μ of the faster one. However, also in this case, η drops for too high values of μ_n and μ_p.

1. The effect of μ on V_{oc} for direct recombination

To understand the difference in the observed trends in η we investigate the characteristic solar cell parameters entering η. We focus on V_{oc} and the FF in the case of $\mu_n = \mu_p$. The short-circuit current density does not give any additional information, because for a constant G_0 it reflects the trend of the FF.

Figure 4 shows V_{oc} and the FF for different recombination models. Comparing the case of a constant β (black crosses) with β_L (red diamonds) shows a different trend in V_{oc}. In the case of Langevin recombination, V_{oc} decreases with μ. This decay results in a drop in η [see Fig. 3(b)] as soon as the increased charge extraction properties seen in the FF cannot overcompensate the V_{oc} loss. This is in contrast to the case of a constant β, where V_{oc} is independent of μ and the monotonous gain with μ in efficiency [see Fig. 3(a)] is due to an increase in FF only. The two curves for constant β and β_L according to Langevin theory cross at $\mu_n = \mu_p = 10^{-4}$ cm^2/Vs because the constant β was chosen to be equal to the Langevin recombination at this mobility. Another constant value of β would simply result in a vertical shift of the black V_{oc} line. To explain the decline in V_{oc} in the Langevin case, we shortly review the origin of V_{oc}.

A photovoltage results from free charge carriers being present and spatially separated. Under the assumption of relaxed charge carriers and selective contacts, V_{oc} is defined as the quasi-Fermi level splitting the solar cell can reach under

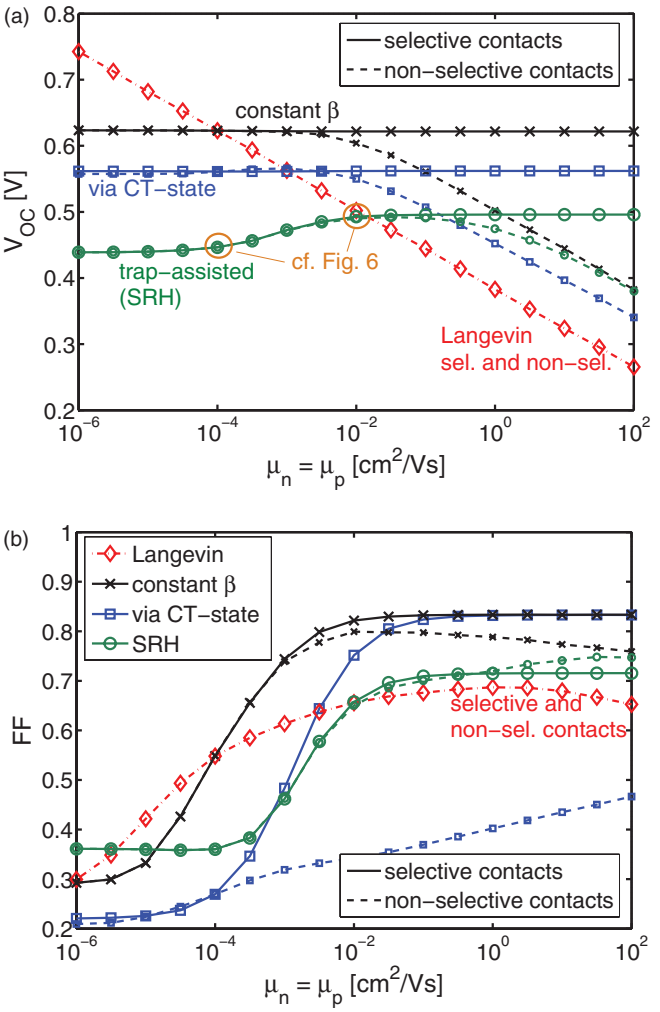

FIG. 4. (Color online) (a) V_{oc} and (b) FF as a function of the mobility $\mu_n = \mu_p$ for different recombination models (symbols) and selective (solid lines) and nonselective contacts (dashed lines). In the case of a constant β, it is chosen to 7.23×10^{-11} cm^{3}s^{-1}, which corresponds to $\beta_L(\mu = 10^{-4}$ cm^2/Vs). The curves for selective and nonselective contacts coincide in case of Langevin recombination, which limits the solar-cell performance in both cases.

illumination without load:[27]

$$eV_{oc} = E_g^{DA} - k_B T \ln \frac{N_C N_V}{np}. \quad (10)$$

Although this equation is only valid for Boltzmann approximation with effective densities of states (N_C and N_V), a comparable equation with possibly modified E_g^{DA} and $N_{C/V}$ describes a similar V_{oc} dependence on np for other distributions of the density of states (DOS) and Fermi-Dirac statistics as well. This was elaborated for a Gaussian DOS in Ref. 28. The central information in Eq. (10) is that V_{oc} increases logarithmically with the product of electron and hole density. Therefore Mandoc *et al.*[8] concluded that a high μ reduced V_{oc} by the reduction of the charge carrier density within the device due to a more efficient extraction. It is correct that a higher μ results in a lower np as long as (drift) current is flowing ($J = en\mu E$), however, not at V_{oc}, because there is by definition no current flowing. Hence, no net-charge extraction occurs.

The data of a mobility independent β (black crosses in Fig. 4) directly contradicts the idea of an enhanced extraction reducing V_{oc}, as V_{oc} does not decrease although charge extraction is strongly increased.

Equation (10) shows that the key expression to understand the dependence of V_{oc} on recombination is given by np, which is calculated self-consistently in the numerical simulation. However, the trends in np can be explained in an intuitive way by analytical equations. That is done with the aid of the continuity equation containing the condition that charge carrier densities can only be changed by generation, recombination, and/or a spatial gradient in the particle current. The continuity equation in steady state reads

$$\frac{\partial p,n}{\partial t} = G_{p,n} - R_{p,n} - \frac{1}{\pm e}\frac{\partial J_{p,n}}{\partial x} = 0. \tag{11}$$

G is the free charge carrier generation rate due to exciton dissociation and J is the current density. An integration of Eq. (11) over the total device thickness d gives under the assumption of a constant generation rate G:

$$\begin{aligned} Gd &= \int_0^d \beta n(x)p(x)dx - [J_p(d) - J_p(0)]/e, \\ Gd &= \int_0^d \beta n(x)p(x)dx + [J_n(d) - J_n(0)]/e. \end{aligned} \tag{12}$$

Here, R is assumed to be of bimolecular type according to Eq. (1) where the intrinsic charge carrier density is neglected since it is much smaller than the photogenerated one.

In case of V_{oc}, the overall current density $J = J_n + J_p$ has to be zero at each x, thus $J_p(x) = -J_n(x)$. Regarding Eq. (11), this means that if a charge carrier flows in one direction, also the inversely charged one flows in the same direction and in sum they recombine with each other. In case of selective contacts, $J_n(0)$ and $J_p(d)$ are zero, thus $J_p(0)$ and $J_n(d)$ are zero as well. This means that all generated charge carriers recombine within the device at V_{oc}. In this situation, there is no reason for large gradients in the hole or electron current. Thus $dJ_{p,n}/dx \approx 0$ and $G \approx \beta np$ hold for each x. Consequently, replacing np in Eq. (10) yields

$$eV_{oc} = E_g^{DA} - k_B T \ln \frac{N_C N_V}{G/\beta}. \tag{13}$$

According to this equation, V_{oc} is influenced by β and decreases with larger values of β. In other words, as G is constant, an increase of β with μ implies a lower np ($G = \beta np$) and thus a lower V_{oc}. This explains that μ, which is not contained in Eq. (13) in the case of a constant β, does not influence V_{oc} [black crosses in Fig. 4(a)].

However, in the case of Langevin recombination, it holds $\beta = \beta_L(\mu)$. This consideration also explains the logarithmic behavior of V_{oc} with μ [red diamonds in Fig. 4(a)], because V_{oc} depends logarithmically on $1/np$, which in turn depends linearly on β and thus on $\mu_n + \mu_p$.

Wang *et al.*[10] attribute the decrease of V_{oc} with μ to dark carrier recombination as a higher μ increases the spreading of dark charge carriers injected from the contacts. These are supposed to recombine with photogenerated charge carriers. We cannot find any evidence for this effect; the data of Fig. 4 visualizes clearly that it is the increase in β that decreases V_{oc}, whereas, an increase in μ in combination with a constant β does not change V_{oc}. This was shown in Ref. 12 by applying a capped Langevin recombination. Furthermore, recombination profiles (cf. Fig. 7) within the device at V_{oc} are homogeneous.

2. *The effect of recombination via CT states on V_{oc}*

In the case of recombination via a CT state (blue squares in Fig. 4) V_{oc} shows a similar behavior with μ as the case of a constant β, although Eq. (2) is applied for β. The FF requires higher mobilities to increase because charge extraction competes with geminate recombination. Choosing $E_B = 350$ meV and $k_{relax} = 10^6\ s^{-1}$, these values result in a V_{oc} of around 0.57 V, which is independent of β and thus of μ also for Langevin recombination.

This independence of V_{oc} on μ was already elaborated by Kirchartz *et al.*[13] within a theoretical detailed balance approach. Here, it is derived as follows. We assume $dJ_{p,n}/dx \approx 0$ in Eq. (11) as previously. Applying Eqs. (3)–(6) gives

$$\begin{aligned} G = G_0 P = R = R_0(1-P) \\ \Rightarrow G_0 = R_0 \frac{1-P}{P} \\ = R_0 \frac{k_{relax}}{k_{diss}} = R_0 \frac{k_{relax}}{\beta e^{-\frac{E_B}{k_B T}} f(E, E_B)}. \end{aligned} \tag{14}$$

The free charge carrier recombination R_0 is given according to Eq. (1). Inserting this equation into Eq. (14) results in

$$G_0 = np \frac{k_{relax}}{e^{-\frac{E_B}{k_B T}} f(E, E_B)}. \tag{15}$$

This equation shows that the generation-recombination equilibrium becomes independent of β. It is dominated by the fraction in Eq. (15), where close to V_{oc} the field dependence gets small. V_{oc} is then governed by the lifetime $1/k_{relax}$ and the energy of the CT state. The radiative lifetime of the CT state determines the maximum efficiency and replaces the radiative lifetime of direct recombination as ultimate limit.[29]

Replacing np in Eq. (10) by Eq. (15) yields

$$\begin{aligned} eV_{oc} &= E_g^{DA} - k_B T \ln \left[\frac{N_C N_V}{G_0} \frac{k_{relax}}{e^{-\frac{E_B}{k_B T}} f(E, E_B)} \right] \\ &= E_g^{DA} - E_B - k_B T \ln \left[\frac{N_C N_V k_{relax}}{G_0 f(E, E_B)} \right]. \end{aligned} \tag{16}$$

Comparing this equation with Eq. (13) reveals a significant difference in the temperature dependence of V_{oc}. Equation (13) predicts a maximum value for V_{oc} at $T = 0$ K of E_g^{DA}/e. Assuming a temperature independent β, a linear extrapolation of V_{oc} results in this maximum value. The slope of $V_{oc}(T)$ is determined by β and by G, which scales with illumination intensity. This is illustrated in Fig. 5 by two curves for different values of β (marker x). In the case of recombination via a CT state [see Eq. (16)], $V_{oc}(T = 0)$ is reduced to $E_g^{DA} - E_B$, which is the energy of the CT state. This approach connects V_{oc}, defined by free charge carriers, with the energy of the

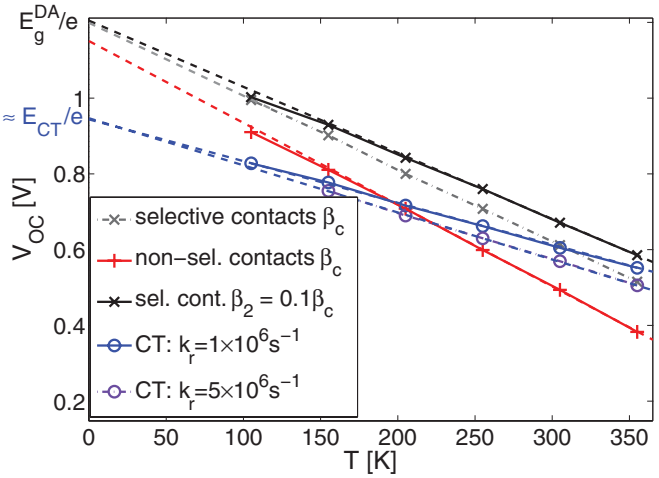

FIG. 5. (Color online) Temperature dependence of the open-circuit voltage V_{oc} for different recombination constants β (x) ($\beta_c = 7.23 \times 10^{-11}$ cm^{3}s^{-1}), CT state lifetimes $1/k_r$ ($E_B = 290$ meV) (o), and nonselective contacts (+) ($\mu = 1$ cm^2/Vs). Dashed lines are linear extrapolations of the 250–350 K region. The slope of $V_{oc}(T)$ depends on the recombination constant β and in case of recombination via CT states on the CT-state lifetime $1/k_r$. $V_{oc}(T \to 0\ \mathrm{K})$ approaches the effective energy gap E_g^{DA} and at recombination via CT states the CT-state energy $E_{CT} = E_g^{DA} - E_B$. In case of significant surface recombination, the extrapolation of V_{oc} to $T = 0$ K does not result in the effective energy gap.

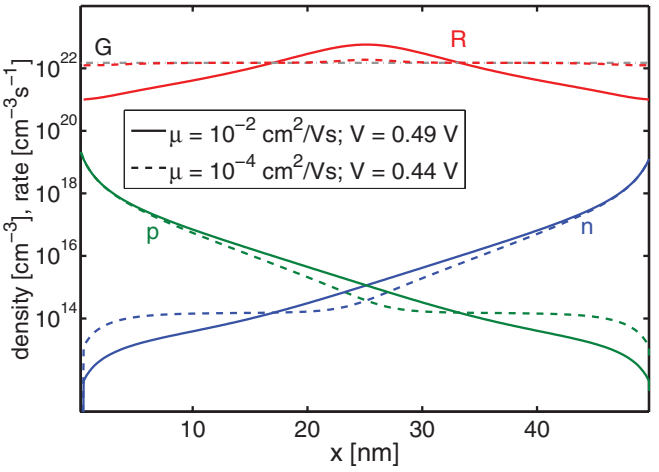

FIG. 6. (Color online) Electron (n) and hole (p) density and the recombination rate (R) within a device, where trap-assisted (SRH) recombination is dominating at V_{oc} of the points marked in Fig. 4 (0.49 V for $\mu = 10^{-4}$ cm^2/Vs, 0.44 V for $\mu = 10^{-2}$ cm^2/Vs). An increased recombination close to the contacts is found for a lower value of μ.

CT state without any additional assumptions. Thus it connects two on first glance completely separate approaches on V_{oc}, which are recently reported and highly debated in literature; one expressing V_{oc} by free charge carrier concentrations and lifetimes that are related to β (see Ref. 30) and the other correlating the CT-state energy with V_{oc} in theory and experiment.[31] Therefore it is not astonishing that both approaches are capable of delivering correct values for V_{oc}.

The slope of $V_{oc}(T)$ is according to Eq. (16) determined by the CT state parameters (circles in Fig. 5). In the case of a distribution of CT states, the independence of V_{oc} of β does not hold any more, which is theoretically elaborated for a two-level system in Ref. 13.

3. *The effect of μ on V_{oc} for trap-assisted recombination*

If one assumes that the capture coefficient c_p in Eq. (7) depends positively on μ like in Langevin theory, a qualitatively identical behavior with μ is expected as for the case of Langevin recombination without CT state or with a CT-state distribution (not explicitly shown): V_{oc} decreases with μ. Setting c_p independent of μ ($N_t c_p = 10^8$ s^{-1}) also results in a small dependence of V_{oc} on μ, however, in this case, with a slight increase of V_{oc} with μ (green circles in Fig. 4). This effect is due to high background majority dark charge carrier concentrations close to the contacts. According to Eq. (8), these charge carrier concentrations result from the low injection barrier at the contacts. Charge carrier density and recombination profiles at V_{oc} are shown in Fig. 6, where two values of μ (10^{-2} and 10^{-4} cm^2/Vs) are chosen. In case of a high mobility (solid lines), the minority charge carriers tend to move toward the middle of the device to reach their low dark (equilibrium) densities close to the contact. Thus the recombination maximum is found in the center of the device. For very low mobilities, charge carrier transport is slower than the recombination process and charge carriers recombine mainly where they are created. This leads to an increased minority density close to the contacts and an increased recombination there, as the dark carrier majority concentration is large at the contacts. The condition for such a redistribution to change V_{oc} is that R in not proportional to np. According to Eq. (7), recombination close to the contacts is approximately proportional to the minority charge carrier density. Another indication for the dark carriers being responsible for the change in V_{oc} is that this effect becomes less pronounced for higher illumination intensity and a lower dark carrier concentration, as shown later on (see Fig. 9).

B. Recombination (also) at electrodes (nonselective contacts)

We now study the case of nonselective contacts, or in other words a surface recombination velocity of infinity also for minorities. Although not always explicitly mentioned, this is the standard case of most of the simulations in literature.[2,10,11] Exceptions are Refs. 12 and 13 where the influence of nonselective contacts was already discussed. We complete the picture by showing ways of a simple experimental determination of this surface-recombination limited case, which is usually expected for a metal/organic interface if no selective charge carrier blocking layers are employed.

Figure 3(d) shows η as a function of μ_n and μ_p under the assumption of a constant β and nonselective contacts. Compared to the case of selective contacts [see Fig. 3(a)], η does not reach a plateau but decays again with higher values of μ. Plots of η for the other recombination models and nonselective contacts are not explicitly shown because they exhibit similar behavior, which means that the shape of η over μ undergoes a decline for high mobilities. Examining V_{oc} and FF shown in Fig. 4 as dashed lines reveals that the reason for

a decrease in η is, again, a decay of V_{oc} with μ. This drop at around 10^{-2}cm^2/Vs is independent of the recombination model. Only for Langevin recombination there is no difference in V_{oc} between selective and nonselective contacts, because bulk recombination is dominating over surface recombination for all μ.

Applying Eq. (12), the reason for the decrease in V_{oc} is found in a negative contribution of $J_{n,p}$, which leads to a decrease of βnp (G constant). For a constant β, this results in a decrease of np and consequently with Eq. (10) in a decline of V_{oc}. The recombination and current profiles displayed in Fig. 7 illustrate this effect. $G = R$, independent of x, which holds for selective contacts (solid lines), is not valid in the case of nonselective contacts and a high μ (dashed lines). R and especially the minority charge carrier densities are lower in the vicinity of the contacts, where recombination is decreased. Although both recombination profiles describe the situation at V_{oc}, where current is zero, the mean recombination rate R is orders of magnitudes lower than the generation rate G in the case of nonselective contacts.

Examining the current profiles [see Fig. 7(b)], one can directly see that this missing recombination is due to equal particle currents of electrons and holes ($J_{tot} = 0$ at every x in steady state V_{oc}) toward the electrodes. This current of electrons and holes in the same direction is diffusion driven by a sink at the contacts. Due to the (conventional and generalized[32]) Einstein relation, diffusion and drift currents increase linearly with μ. If there is a sink present also at the "wrong" electrode, a higher μ causes more (minority) charge carriers to diffuse to this "wrong" electrode where they do not contribute to V_{oc}, but are lost.

If bulk recombination is negligible, the solar cell works in a completely diffusion limited mode, which means that all charge carrier losses are due to diffusion to the "wrong" contact. Only in such a situation is the analytical equation of Sokel and Hughes[33] applicable, which is often used to describe experimental photocurrents.[20] Evidence for this case being present in experiment is given if the photocurrent, as difference between dark current and current under illumination, is extracted in forward direction as well. This requires a crossing of the J-V curve under illumination and the dark J-V curve. In the previously discussed case of selective contacts, this equation of Sokel and Hughes is not applicable because all generated charges recombine at V_{oc}.

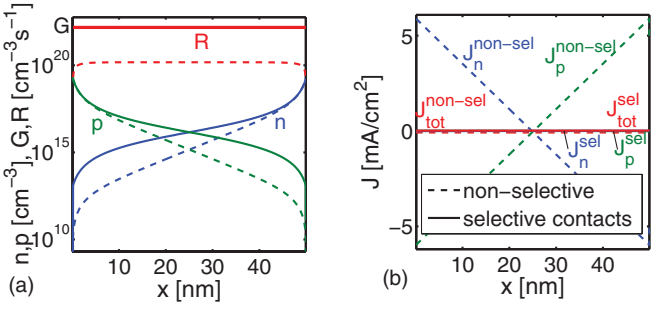

FIG. 7. (Color online) (a) Charge carrier density and (b) current profiles at V_{oc} for selective (solid lines, $V_{oc} = 0.62$ V) and nonselective contacts (dashed lines, $V_{oc} = 0.50$ V). Here, $\beta = 7.23 \times 10^{-11}$ cm^{3}s^{-1} and $\mu = 1$ cm^2/Vs.

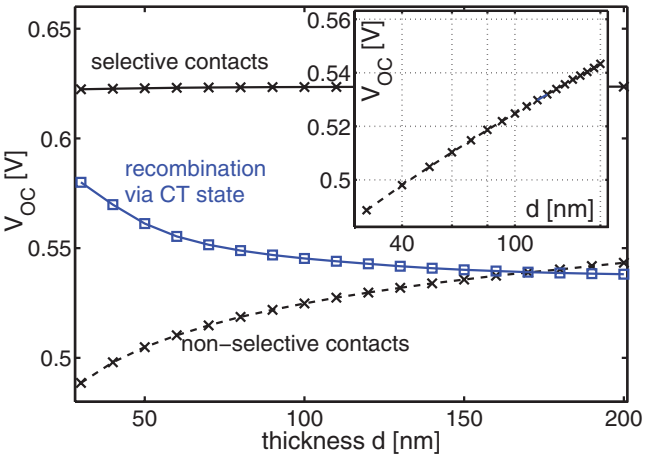

FIG. 8. (Color online) Thickness dependence of V_{oc} in the case of selective contacts ($\mu = 10^{-4}$ cm^2/Vs), nonselective contacts and $\mu = 1$ cm^2/Vs, and for recombination via CT states. In all cases G is constant and $\beta = 7.23 \times 10^{-11}$ cm^{3}s^{-1}. The inset shows the logarithmic increase of V_{oc} with d in case of nonselective contacts.

As diffusion is temperature activated, this effect is expected to be more pronounced for higher T. The red dashed line (+) in Fig. 5 shows indeed a stronger decrease in V_{oc} with T compared to the reference with selective contacts (solid black line, x). Therefore, if surface recombination is significant, an extrapolation of $V_{oc}(T)$ to $T = 0$ K does not result in E_g^{DA}, but in a lower value.

Another indication for the diffusion loss can be found in an examination dependent on the thickness of the bulk heterojunction layer. Figure 8 shows a comparison of the dependence of V_{oc} on the BHJ thickness d dependent on the dominating recombination mechanism. For selective contacts V_{oc} is according to Eq. (10) independent of d. In the case of recombination at the contacts V_{oc} increases logarithmically with d (additionally visualized in the inset), which can be explained by the fact that the field in the device decreases approximately linearly with device thickness ($E \approx V/d$). This means that the drift current ($J \propto E$), which is at V_{oc} balanced by a diffusion current, decreases linearly with d. Since the diffusion current is proportional to the diffusion gradient, the total diffusion gradient decreases linearly with d as expected. A decreased diffusion gradient corresponds to a decreased gradient in the quasi-Fermi levels, which are logarithmically related to charge carrier densities. Thus a diffusion current creates a voltage, which scales logarithmically with the current, as, e.g. known from the ideal diode equation.[23] Therefore this diffusion voltage which is reverse to V_{oc} decreases logarithmically with d and leads to the observed increase in V_{oc}. Figure 8 also shows V_{oc} as a function of d for recombination via CT states where the trend is inverse to surface recombination. The reason for this behavior is found in the expression $f(E, E_B)$ in Eq. (16). This equation shows that V_{oc} decreases with d if the CT state dissociation depends on the electrical field E which decreases with increased layer thickness for a certain voltage. This effect is only expected to be significant if $V_{bi} > V_{oc}$ so that there is a significant field in the device at V_{oc}.

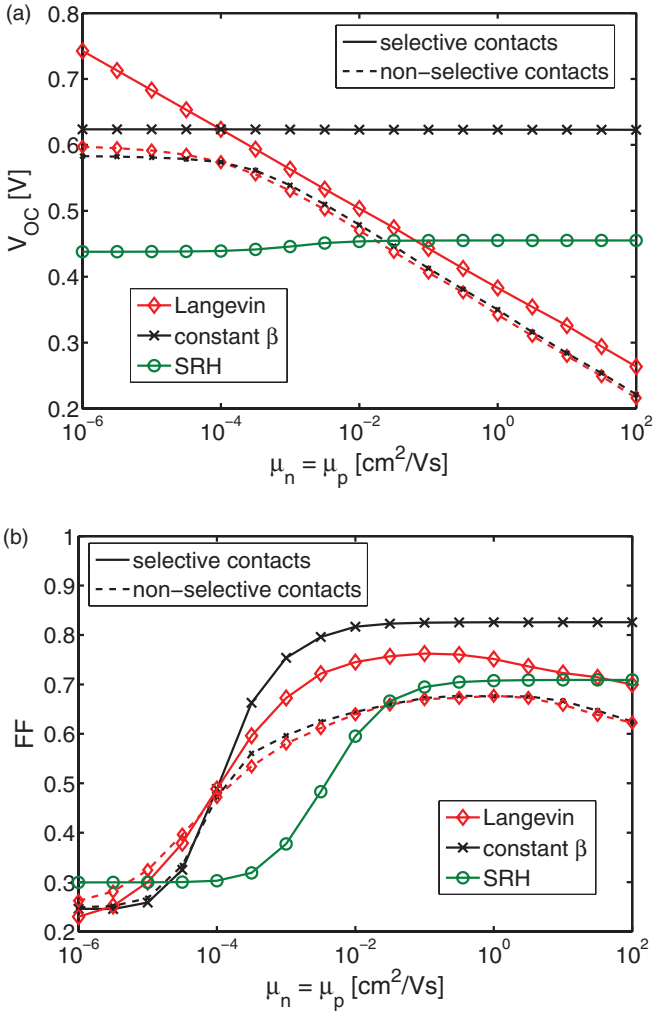

FIG. 9. (Color online) (a) V_{oc} and (b) FF as a function of the mobility $\mu_n = \mu_p$ in the cases of an injection barrier of 0.3 eV. V_{oc} remains unchanged compared to Fig. 4 in the case of selective contacts (solid lines), whereas nonselective contacts (dashed lines) reduce V_{oc} and FF.

The dependence of V_{oc} on d can be taken as a simple experimental proof to determine the dominating recombination process. It is important to adjust the light intensity to get a constant averaged generation rate G, which can be seen in a constant ratio between photocurrent and d. An increase of V_{oc} for higher thicknesses then implies charge carrier losses at the wrong contact, whereas a decrease of V_{oc} with d might indicate the presence of losses via geminate recombination.

Considering the logarithmic decay of V_{oc} with d, a similar explanation holds for the decay with μ seen at the dashed lines of Fig. 4(a) in the surface recombination limited case. As the total diffusion gradient is fixed by the charge carrier densities at the contacts according to Eq. (8), the diffusion losses are proportional to μ and, therefore, cause a voltage loss which depends logarithmically on μ.

We conclude that also in the case of nonselective contacts, the increase of the transport parameter μ itself does not decrease V_{oc}. It is the indirect effect of μ being an enhancement factor of surface recombination. In experiments, the qualitative effect of selective and nonselective contacts is well known and

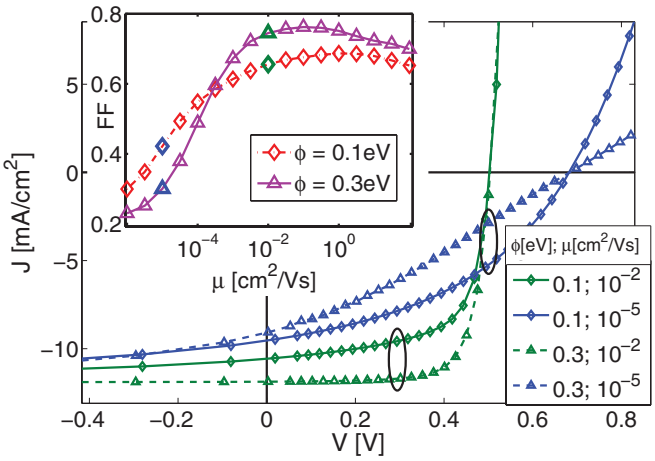

FIG. 10. (Color online) J-V curves for two different mobilities (10^{-2} and 10^{-5} cm^2/Vs), Langevin recombination, and selective contacts. The injection barriers are 0.1 eV (solid lines, diamonds) and 0.3 eV (dashed, triangles). The inset compares the dependence of the FF on μ for the two barrier heights.

seen in, e.g., an enhancement of V_{oc} of BHJs by the addition of a (selective) interlayer between metal and the BHJ.[34,35] This explains that very high values for V_{oc} of a ZnPc:C_{60} BHJ are reported for devices where the blend is sandwiched between wide-gap transport layers[17] in a p-i-n architecture.[35] In this structure, minority charge carriers cannot penetrate the charge transport layers. However, a large amount of molecular dopant adjacent to the BHJ could be a source of minority charge carrier recombination, decreasing the selectivity property of the contact. A planar heterojunction contains this selectivity already as a built-in property.[3]

C. Injection barriers

As the influence of the metal work function in experiment, corresponding to the injection barrier height in simulation, is still under discussion, we perform the same mobility dependent study for an increased injection barrier ($\varphi = 0.3$ eV). A higher barrier results in two effects: first, according to Eq. (8), the majority charge carrier densities at the contacts are reduced. Second, according to Eq. (9), the built-in field is reduced. The following discussion focuses on the effect of these changes dependent on the selectivity of the contacts.

1. Selective contacts

In the case of selective contacts and direct recombination, the barrier and, thus, in the thermionic injection model, the dark carrier concentrations, are not relevant for V_{oc} because they do not introduce an additional source of recombination (solid lines in Fig. 9). V_{oc} can even exceed V_{bi} (0.6 V) if the contacts are selective. Thus the statements made above for $\varphi = 0.1$ eV still hold.

Although the trend of the FF is the same with and without significant barrier, the inset of Fig. 10 shows a remarkable change of the FF in the case of Langevin recombination. For low mobilities, the FF is reduced by a higher φ due to a stronger dependence of the charge carrier collection on the applied bias caused by a decreased built-in field [see Fig. 11(a)]. This results in a higher recombination in the center of the device

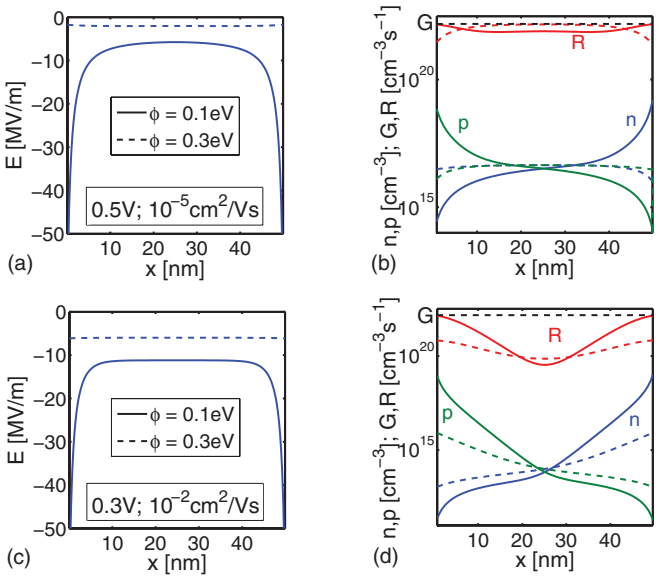

FIG. 11. (Color online) Electric field and charge carrier density profiles under the conditions marked in Fig. 10 (Langevin recombination, selective contacts, and varied φ): (a) and (b) $V = 0.5$ V and $\mu = 10^{-5}$ cm^2/Vs, (c) and (d) $V = 0.3$ V and $\mu = 10^{-2}$ cm^2/Vs.

[dashed in Fig. 11(b)] and in an S-kinked J-V curve because the current is mainly diffusion driven.[3]

For high mobilities, the FF is higher for a larger φ. The reason is that the drift current providing charge carrier extraction is sufficient also for the lower built-in field. At the same time the recombination within the device is higher for a lower ϕ. This is shown in Figs. 11(c) and 11(d), visualizing the high majority charge carrier densities close to the contacts, which result from a lower ϕ. This background dark carrier density increases the recombination probability of photogenerated minorities close to the contacts. Once more, this change in recombination does not influence V_{oc} as it shows only effect as long as there is charge carrier extraction by a current.

In Fig. 9, $V_{oc}(\mu)$ is also plotted for SRH recombination. The plot shows that V_{oc} is less dependent on μ compared to the case of a lower φ (see Fig. 4). The reason is a reduced dark carrier concentration close to the contacts due to the increased injection barriers.

2. *Nonselective contacts*

In the case of nonselective contacts, η is generally lower with a higher φ. The reason is a decrease in V_{oc} compared to devices with a lower φ (dashed lines in Fig. 9). The diffusion to the "wrong" electrode becomes already relevant at lower positive bias voltages because of the lower built-in field. Consequently, one can distinguish two limiting regimes in $V_{oc}(\mu)$ in such a high-barrier case: on the one hand, the contact work function can directly limit V_{oc}, which happens if eV_{bi} is lower than the maximum possible quasi-Fermi level splitting in the blend caused by illumination. This is the case for low mobilities (up to 10^{-4} cm^2/Vs) in Fig. 9 and results in an only small dependence of V_{oc} on μ splitting in the blend caused by illumination. Such a behavior was observed in the simulation results of Refs. 10 and 11, however, it has not been identified as such.

On the other hand, for higher μ ($>10^{-4}$ cm^2/Vs), the diffusion or in the case of Langevin recombination possibly bulk recombination is limiting, which lead to a decrease of V_{oc} with μ. The coincidence of $V_{oc}(\mu)$ for Langevin theory and a constant β ($\mu > 10^{-4}$ cm^2/Vs in Fig. 9) below the Langevin curve for selective contacts indicates that the recombination losses at the surface dominate in this case.

D. Effect of energy-level bending on V_{oc}

To complete the discussion about V_{oc}, charge transport level bending ($\Delta\varepsilon_B$) close to the contacts is discussed (inset of Fig. 12). In literature, this bending is suggested[36] and several times ascribed[37] as loss mechanism for V_{oc}, because it reduces the field in the device to a value $(V_{bi} - \Delta\varepsilon_B/e)/d$. The reason for the bending is the space charge at the electrodes due to the high majority charge carrier density there [cf. Eq. (8)]. This density approaches its maximum in the case of Ohmic contacts where the Fermi level reaches the charge transport level ($\varphi = 0$).

The space charge at the electrodes and hence the bending can directly be influenced by changing $N_{C,V}$ [cf. Eq. (8)] without changing V_{bi}. The increase of $\Delta\varepsilon_B$ with increased $N_{C,V}$ is shown in Fig. 12 together with V_{oc}. Although both show the same trend, the change of V_{oc} is independent of φ. However, $\Delta\varepsilon_B$ increases with a lower φ. Thus V_{oc} does not correlate directly with $\Delta\varepsilon_B$. The effect of $N_{C,V}$ on V_{oc} can directly be seen in Eq. (10), where an increased $N_{C,V}$ reduces V_{oc} at a constant np because there are more low-energy states to be filled first. Thus this is the origin of the change in V_{oc} with $N_{C,V}$. The bending itself is only a concomitant phenomenon, which can be seen at very high $N_{C,V}$, although V_{oc} scales for all $N_{C,V}$. This leads to the conclusion that an Ohmic contact does not reduce V_{oc}. Ohmic and selective contacts are perfect for any type of solar cell.[27]

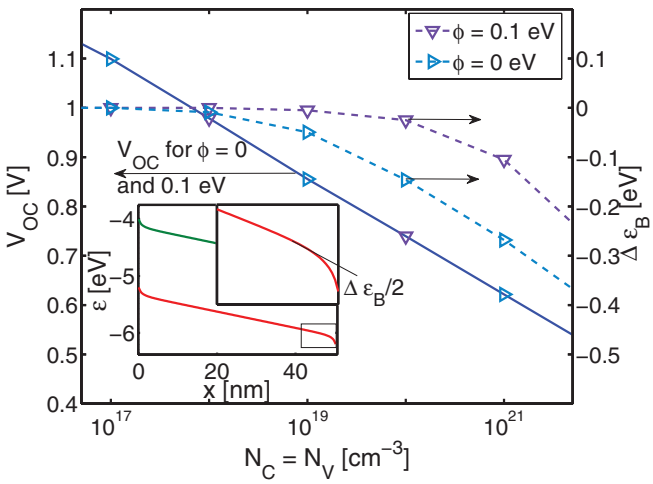

FIG. 12. (Color online) V_{oc} as a function of the effective densities of states $N_C = N_V$ and the amount of potential drop $\Delta\varepsilon_B$ due to bending of the energy levels at the contacts as depicted in the inset. V_{oc} is independent of φ and does not directly correlate with $\Delta\varepsilon_B$. The contacts are assumed to be selective and $\beta = 7.23 \times 10^{-11}$ cm^{3}s^{-1}. The inset shows an energy-level diagram visualizing the bending of the energy levels $\Delta\varepsilon_B/2$ close to each contact due to high charge carrier densities there.

IV. CONCLUSIONS

We have shown that the results of simple drift-diffusion simulations and, especially, the existence of an optimum mobility depend strongly on the assumptions made for bulk and surface recombination. We clarified that selective Ohmic contacts are the optimum choice, also for organic solar cells. Then, V_{oc} is limited by recombination in the device and depends only on μ in the case of recombination processes, where the recombination constants are a function of μ (Langevin recombination), or if $R \propto np$ is not given like in SRH recombination. If free charge carrier generation and recombination happen through a CT state, V_{oc} is governed by the dynamics of this state rather than by free-charge carrier recombination coefficients. Furthermore, barriers at the electrode and dark carrier concentrations in combination with varied mobilities do not alter V_{oc} in the case of direct/bimolecular recombination.

Only if the contacts are nonselective, an additional loss path arises by the extraction of charge carriers at the "wrong" electrode. Then V_{oc} is decreased by injection barriers or by a very high mobility itself, as both, the first one by a lower built-in field and the second one by a higher diffusivity increase this diffusion loss. The case of this surface recombination limit is expected to be seen in experiment by a V_{oc} that depends on layer thickness. In conclusion, this study contributes to a better understanding of experimental data and to a careful and profound interpretation of outputs of simulations.

ACKNOWLEDGMENTS

W.T. thanks the Reiner Lemoine foundation for funding. Additional support from BMBF (OPEG, 13N9720) is gratefully acknowledged. The authors thank Jan Meiss, Johannes Widmer, and David Wynands for carefully reading the manuscript and Thomas Kirchartz for discussions.

*wolfgang.tress@iapp.de

[1] M. A. Green, K. Emery, Y. Hishikawa, W. Warta, and E. D. Dunlop, Progr. Photovoltaics **20**, 12 (2012).
[2] L. J. A. Koster, E. C. P. Smits, V. D. Mihailetchi, and P. W. M. Blom, Phys. Rev. B **72**, 085205 (2005).
[3] W. Tress, K. Leo, and M. Riede, Adv. Funct. Mater. **21**, 2140 (2011).
[4] C. W. Tang, Appl. Phys. Lett. **48**, 183 (1986).
[5] M. Hiramoto, H. Fujiwara, and M. Yokoyama, Appl. Phys. Lett. **58**, 1062 (1991).
[6] G. Yu, J. Gao, J. C. Hummelen, F. Wudl, and A. J. Heeger, Science **270**, 1789 (1995).
[7] J. J. M. Halls, C. A. Walsh, N. C. Greenham, E. A. Marseglia, R. H. Friend, S. C. Moratti, and A. B. Holmes, Nature **376**, 498 (2002).
[8] M. M. Mandoc, L. J. A. Koster, and P. W. M. Blom, Appl. Phys. Lett. **90**, 133504 (2007).
[9] C. Deibel, A. Wagenpfahl, and V. Dyakonov, Phys. Status Solidi **2**, 175 (2008).
[10] Y.-X. Wang, S.-R. Tseng, H.-F. Meng, K.-C. Lee, C.-H. Liu, and S.-F. Horng, Appl. Phys. Lett. **93**, 133501 (2008).
[11] J.-T. Shieh, C.-H. Liu, H.-F. Meng, S.-R. Tseng, Y.-C. Chao, and S.-F. Horng, J. Appl. Phys. **107**, 084503 (2010).
[12] A. Wagenpfahl, C. Deibel, and V. Dyakonov, IEEE J. Sel. Top. Quantum Electron. **16**, 1759 (2010).
[13] T. Kirchartz, B. E. Pieters, K. Taretto, and U. Rau, Phys. Rev. B **80**, 035334 (2009).
[14] P. Langevin, Ann. Chim. Phys.**VII**, 433 (1903).
[15] W. F. Pasveer, J. Cottaar, C. Tanase, R. Coehoorn, P. A. Bobbert, P. W. M. Blom, D. M. de Leeuw, and M. A. J. Michels, Phys. Rev. Lett. **94**, 206601 (2005).
[16] L. J. A. Koster, V. D. Mihailetchi, and P. W. M. Blom, Appl. Phys. Lett. **88**, 052104 (2006).
[17] W. Tress, S. Pfuetzner, K. Leo, and M. Riede, J. Photon. Energy **1**, 011114 (2011).
[18] L. Onsager, Phys. Rev. **54**, 554 (1938).
[19] C. L. Braun, J. Chem. Phys. **80**, 4157 (1984).
[20] V. D. Mihailetchi, L. J. A. Koster, J. C. Hummelen, and P. W. M. Blom, Phys. Rev. Lett. **93**, 216601 (2004).
[21] M. M. Mandoc, F. B. Kooistra, J. C. Hummelen, B. De Boer, and P. W. M. Blom, Appl. Phys. Lett. **91**, 263505 (2007).
[22] R. A. Street, M. Schoendorf, A. Roy, and J. H. Lee, Phys. Rev. B **81**, 205307 (2010).
[23] S. M. Sze, *Physics of Semiconductor Devices*, 2nd ed. (Wiley, New York, 1981).
[24] J. D. Kotlarski, D. J. D. Moet, and P. W. M. Blom, J. Polym. Sci., Part B: Polym. Phys. **49**, 708 (2011).
[25] V. D. Mihailetchi, J. Wildeman, and P. W. M. Blom, Phys. Rev. Lett. **94**, 126602 (2005).
[26] W. Tress, A. Petrich, M. Hummert, M. Hein, K. Leo, and M. Riede, Appl. Phys. Lett. **98**, 063301 (2011).
[27] P. Würfel, *Physics of Solar Cells: From Basic Principles to Advanced Concepts* (Wiley-VCH, Weinheim, 2009).
[28] G. Garcia-Belmonte, Sol. Energy Mater. Sol. C. **94**, 2166 (2010).
[29] W. Shockley and H. J. Queisser, J. Appl. Phys. **32**, 510 (1961).
[30] A. Maurano, R. Hamilton, C. G. Shuttle, A. M. Ballantyne, J. Nelson, B. O'Regan, W. Zhang, I. McCulloch, H. Azimi, M. Morana, C. J. Brabec, and J. R. Durrant, Adv. Mater. **22**, 4987 (2010).
[31] K. Vandewal, K. Tvingstedt, A. Gadisa, O. Inganäs, and J. V. Manca, Phys. Rev. B **81**, 125204 (2010).
[32] Y. Roichman and N. Tessler, Appl. Phys. Lett. **80**, 1948 (2002).
[33] R. Sokel and R. C. Hughes, J. Appl. Phys. **53**, 7414 (1982).
[34] C. J. Brabec, S. E. Shaheen, C. Winder, N. S. Sariciftci, and P. Denk, Appl. Phys. Lett. **80**, 1288 (2002).
[35] B. Maennig, D. Gebeyehu, P. Simon, F. Kozlowski, A. Werner, F. Li, S. Grundmann, S. Sonntag, M. Koch, K. Leo, M. Pfeiffer, H. Hoppe, D. Meissner, N. S. Sariciftci, I. Riedel, V. Dyakonov, J. Parisi, and J. Drechsel, Appl. Phys. A **79**, 1 (2004).
[36] V. D. Mihailetchi, P. W. M. Blom, J. C. Hummelen, and M. T. Rispens, J. Appl. Phys. **94**, 6849 (2003).
[37] D. Veldman, S. C. J. Meskers, and R. A. J. Janssen, Adv. Funct. Mater. **19**, 1939 (2009).